

A novel multi-jet quartz burner for laminar near-adiabatic flames: Standard of temperatures for the calibration of laser diagnostics techniques

Bo Li¹, Yu Li (presenter)¹, Zhihua Wang², Zhongshan Li^{1*}, Zhiwei Sun¹, Marcus Aldén¹

¹Division of Combustion Physics, Lund University, Box 118, S-221 00 Lund, Sweden

²Institute for Thermal Power Engineering, Zhejiang University, Hangzhou, 310027, P. R. China

Abstract

We demonstrate a novel multi-jet quartz burner which was used as a calibration burner in stabilizing near adiabatic flat flames at atmospheric pressure with variable temperatures. Compared with metal-made burners, this quartz burner provides cleaner and near to adiabatic flames owing to less heat sink to the burner surface. In this work, premixed CH₄/Air flame was investigated to provide adiabatic laminar flame at different temperatures. Single shot 2D OH planar laser induced fluorescence (PLIF) was applied to investigate the instantaneous flow field of the flame, making sure that the flame is laminar, and validating the accumulation method adopted later on. A 2D Rayleigh scattering thermometry was carried out over the entire flame to measure the temperatures for different flame conditions. The errors of the results were analyzed. The results indicate that the burner presented here can be used to provide clean, reliable and handy calibration flames for testing new optical diagnostic techniques.

1. Introduction

In the past decades laser based diagnostic techniques have played a key role in combustion research by providing non-intrusive, in-situ measurements of temperature, velocity and individual molecular species concentrations with high spatial and temporal resolution [1]. For calibration and validation of new laser spectroscopic techniques, standard flames with known temperature distribution are always important in laser combustion diagnostics labs. Two-line atomic LIF thermometry technique [2], for instance, needs to be calibrated by a burner with known temperature prior to being utilized in other situations. Calibration burner is needed for this purpose, which possesses the following merits. 1. It can provide stable laminar flames with uniform region in terms of temperature, both spatially and temporally; 2. Different techniques can be easily applied in it, such as point measurement techniques and 2D imaging techniques; 3. It can generate flames with a wide variation of the stoichiometry. A few burners have been developed for this purpose.

McKenna Burner [3] is probably the most frequently-used calibration burner. It has a water-cooled porous plate, which favors stabilizing premixed laminar flames, but at the same time makes it not feasible for being applied in tracer seeded techniques. The cooling water adds complexity and inconvenience to the experimental setup. Other calibration burners, such as the commercially available Hecken burner [4], and recently designed flat flame burner [5] suffer from their complexity as well. Besides, most of the calibration burners, including the ones mentioned above, are made of metal materials, which will introduce contamination to the flame owing to metal evaporation at high

temperature. In addition, the metal burners, especially the micro structures on the burner plate, tend to distort because of the stress accumulation and release under the drastically changed temperature. And once the metal burner was contaminated by carbon deposited or tracer seeded, it is hard to be cleaned. Finally, the high thermal conductivity of metal materials leads to a high heat sink from the flame being stabilized on such burners, which will consequently enlarges the temperature difference between the real flames and adiabatic ones.

Hence, a novel multi-jet quartz burner was adopted in this paper in generating flat flames for calibration of different laser spectroscopic techniques. Stable adiabatic flames can be easily produced on this burner with controllable temperatures. Line-of-sight techniques, 2D imaging techniques, and tracer seeded techniques can be easily applied on this burner. The burner is compact and simple, and thus is convenient for applications. Compared with metal-made burners, this quartz burner provides cleaner and near adiabatic flames due to the less heat sink to the burner surface. And its distortion is negligible after long term of working. And it can be easily cleaned by chemicals after contamination by either deposited carbon or seeded tracer species.

2. Rayleigh scattering theory

2.1 Rayleigh scattering thermometry

Laser Rayleigh scattering is a powerful tool for determining flame temperatures, and simpler as well compared with other laser thermometry techniques. Rayleigh scattering is an elastic scattering of photons from atoms, molecules, or other particles that are

*Corresponding author: zhongshan.li@forbrf.lth.se

smaller compared to the wavelength of incident light. The total intensity of Rayleigh scattering can be expressed as

$$I_R = CI_0N\sigma_{eff} \quad (1)$$

All the symbols in the equation are explained as follows.

- I_R -Rayleigh scattering intensity;
- C -constant that describing the detector sensitivity, signal collection efficiency, and probe volume;
- I_0 -incident light intensity;
- N -total number density of the gas mixture;
- σ_{eff} -effective Rayleigh scattering cross section of the gas mixture.

The σ_{eff} can be calculated as:

$$\sigma_{eff} = \sum_i \chi_i \sigma_i, \quad (2)$$

where χ_i and σ_i are the mole fraction and Rayleigh scattering cross section of the i th species, respectively.

Assuming that we are measuring two gases, pure nitrogen at room temperature and burned gas in the laminar methane/air flame, by the same experimental setup, we can then deduce equation (3) since C and I_0 is the same for both gases in equation (1).

$$\frac{I_{R-nitrogen}}{I_{R-burned\ gas}} = \frac{N_{nitrogen} \sigma_{nitrogen}}{N_{burned\ gas} \sigma_{eff-burned\ gas}} \quad (3)$$

If we also know that both gases are measured at atmospheric pressure, then according to ideal gas law, equation (4) will be derived.

$$\frac{N_{nitrogen}}{N_{burned\ gas}} = \frac{T_{burned\ gas}}{T_{nitrogen}} \quad (4)$$

Then combining equation (3) and (4) will deduce:

$$T_{burned\ gas} = T_{nitrogen} \frac{I_{R-nitrogen}}{I_{R-burned\ gas}} \frac{\sigma_{eff-burned\ gas}}{\sigma_{nitrogen}} \quad (5)$$

In equation (5), $T_{nitrogen}$ is room temperature, Rayleigh scattering intensity for both gases can be measured, $\sigma_{nitrogen}$ is known, and $\sigma_{eff-burned\ gas}$ can be calculated by equation (2) (in the burned gas of laminar methane/air flames, Rayleigh scattering cross section for major species is known, and the mole fraction of different species can be precisely calculated out by CFD software, such as FLUET). So we will finally obtain the temperature of the burned gas of laminar methane/air flame.

2.2 Rayleigh scattering cross section

Cross section of main products of a methane/air flame with an incident laser wavelength of 532 nm is shown in Tab 1. [6, 7] In this paper, only main products have been taken into consideration, and according to Gavin *et al.* [8], the contributions from other species in the burned gas, like OH, are negligible.

Table 1. Cross section of main products of methane/air flame with an incident laser wavelength of 532 nm.

	O ₂	N ₂	H ₂	CO ₂	CO	H ₂ O
σ (10 ⁻²⁸ cm ²)	5.08	6.13	1.34	7.87	13.8	4.43

3. Apparatus and experimental procedure

3.1 Multi-jet quartz burner

The structure of the multi-jet burner is shown in Fig. 1. The multi-jet burner is made of quartz, and the gas flow can be divided into two parts, jets and dilute-flow. There are as many as 40 jets (1 mm in inner diameter and 3 mm in outer diameter) evenly distributed in the dilute-flow tube (24 mm in inner diameter). The surface of the jets is 4 mm lower than that of the dilute tube.

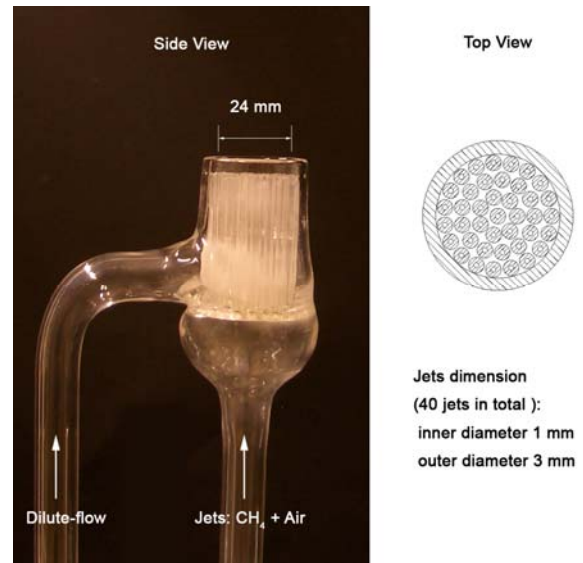


Figure 1. Structure of multi-jet burner.

Premixed methane/air gas was introduced into the jets. And since the diameter of the jets is smaller than the quenching distance of premixed methane/air flame, flashback is prevented. Nitrogen, argon or any other inert gas can be introduced into the dilute-flow tube to regulate the temperature of the outer flame.

By varying the equivalence ratio of the jets gas, dilute gas and their flow rates, one can easily produce different premixed flames with different temperatures on the quartz burner.

Further more, all kinds of tracers can be easily seeded into the flame through either the multi-jets or the dilute-flow tube if it is necessary, and the residue of the

tracers will be totally removed from the burner afterwards.

In this experiment, all the gases were controlled by thermal mass flow controllers (Bronkhorst High-Tech B.V., EL-FLOW series) with the accuracy of $\pm 0.8\%$ Rd plus $\pm 0.2\%$ FS, which has been recently calibrated by the manufacturer.



Figure 2. Photo of a stoichiometric methane/air laminar flame stabilized on the multi-jet quartz burner.

Fig. 2 shows a stoichiometric methane/air laminar flame stabilized on the burner with nitrogen as dilute-flow. It can be seen in the figure that in the cavity beneath the surface of the dilute-flow tube, there are flames attached on top of each jet. And we were measuring in the uniform burned gas region, which is higher than the burner surface.

3.2 Laser systems

OH PLIF and laser Rayleigh scattering measurements were carried out separately. Single shot OH PLIF was applied firstly to investigate the instantaneous flow field of the flame, making sure that the flame is laminar, and validating the accumulation method adopted by laser Rayleigh scattering technique later on. Then 2D laser Rayleigh scattering thermometry was carried out over the burned gas region of the flame to measure the temperatures for different flame conditions.

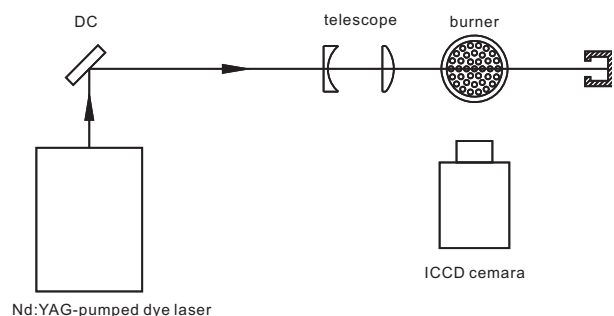


Figure 3. Laser system for OH PLIF and 2D Rayleigh scattering measurements.

3.2.1 OH PLIF setup

The OH PLIF setup is illustrated in Fig. 3. A Nd:YAG (Spectra-Physics, PRO 290-10) pumped dye laser (Continuum, ND60) system was employed to detect OH molecules in the flame. The dye laser was working with Rhodamine 590, and was tuned to around 283nm after frequently doubling. Then after telescope lens and a slit aperture, a laser sheet formed 5 mm above the quartz burner.

PLIF of OH molecules was collected by an ICCD camera (Princeton PI-MAX, 512x512 pixels) with a UV-transmitted objective (B-Halle, UV objective, $f = 100$ mm, $f_{\text{number}} = 2$). In order to block the scattered laser, an interference filter at 310 nm (with band width of 15 Å) was mounted on the objective.

The dye laser for OH excitation was tuned to the $Q_1(5)$ line in $A^2\Sigma^+ \leftarrow X^2\Pi_i(1,0)$ band of OH at 282.667 nm (in air). And the laser was running at 10 Hz with laser energy of around 10 mJ per pulse.

Sequent single shot images were saved by the camera for different flame conditions.

3.2.2 Laser Rayleigh scattering setup

The laser Rayleigh scattering set-up is shown in Fig. 3 as well. The 532 nm laser, second harmonic output from the same Nd:YAG laser system, was employed to detect Rayleigh scattering in the flame. After going through a pair of telescope lens and a slit aperture, a laser sheet was formed 5 mm above the quartz burner.

The Rayleigh scattering signal was collected by an $f/1.2$ objective (Nikon, $f = 50$ mm), and then captured by the same ICCD camera mentioned above. No filter was used this time. The gating width and gain were typically 30 ns and 200, respectively.

The laser was running at 10 Hz with laser energy of around 400 mJ per pulse.

For each measurement, 500 times of accumulation has been performed by the camera. And the laser Rayleigh scattering accumulation image of pure nitrogen (at room temperature) and the flames have been measured alternatively to eliminate the influence of the laser fluctuation.

4. Results and discussion

4.1 Single shot images of OH PLIF

Single shot OH PLIF image of a premixed methane/air flame with the equivalence ratio of 0.9 is shown in Fig. 4. It can be seen that the flame is laminar, and OH molecules are uniform over the entire burned gas region. So it is reasonable of performing accumulation by the ICCD camera when collecting Rayleigh scattering signal.

4.2 Laser Rayleigh scattering thermometry

4.2.1 Validation measurements

In Rayleigh scattering measurements, there is no wavelength shift between signal light and incident laser,

and accordingly, no filter can be applied on the camera to remove the stray laser light from optical components, especially from the quartz burner itself. So it is very important to find out the contribution from this stray laser light to the ICCD camera. Hence, the validation experiments were performed prior to the temperature measurements.

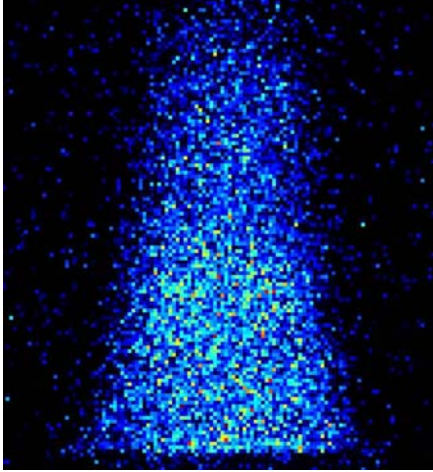


Figure 4. Single shot OH PLIF image of a premixed methane/air flame with the equivalence ratio of 0.9.

Pure methane and pure nitrogen at 300 K were introduced into the burner alternatively, and Rayleigh scattering measurements were carried out on both gases, respectively. According to the Rayleigh scattering theory, the Rayleigh scattering signal ratio for two gases should be equal to the ratio of their differential cross sections. Since we know the differential cross sections with an incident wavelength of 532 nm at 300 K to be $13.42 \times 10^{-28} \text{ cm}^2$ for methane, and $6.13 \times 10^{-28} \text{ cm}^2$ for nitrogen, respectively, their ratio is calculated to be 2.19, while the experimental results give a ratio of 2.19 ± 0.01 . The difference is lower than 0.5%, and is within the uncertainty of the experiments.

4.2.2 Rayleigh scattering signal from different flame conditions

In this paper, the flow speed of the supply gas (premixed methane/air) through the jets is fixed at 1 m/s and 1.5 m/s, 1.88 l/min and 2.83 l/min, respectively. For each flow speed, four flames with equivalence ratio varying from 0.7 to 1.0 were measured by Rayleigh scattering. The main results are shown in Fig. 5 and Fig. 6.

Fig. 5 shows the equivalence ratio dependence of the temperature measured at 10 mm the height above the burner (HAB) in different flames. The adiabatic flame temperature for different equivalence ratio is also plotted as reference.

It can be seen from Fig. 5 that all the measured temperature is lower than the adiabatic flame. This is supposed to be the case, considering that in a real flame, heat sink to the burner as well as the thermal radiation to the ambient air happens all the time.

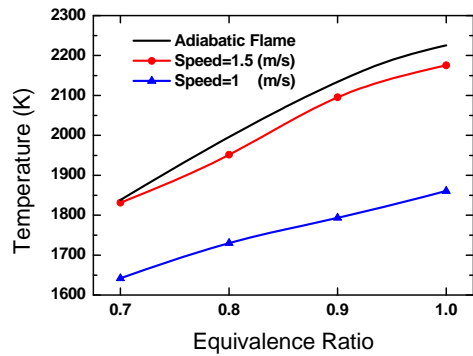


Figure 5. The equivalence ratio dependence of the temperature measured for different flames (10 mm above the burner), as well as the temperature calculated for adiabatic flame.

Another fact is that the flame with higher gas supply speed has a higher temperature, closer to the adiabatic flame case. This could be explained as follows. When the gas supply speed is higher, the flame will “jump” higher accordingly, leading to less heat sink to the burner, which finally decreases the flame temperature.

And it has been noticed that by changing the flame parameters, the temperature of the burned gas can be varied from $\sim 2200 \text{ K}$ to $\sim 1600 \text{ K}$ at HAB of 10 mm, and if the dilute flow is introduced, the temperature can be even lower. So the multi-jet quartz burner can provide different temperatures needed in a large range.

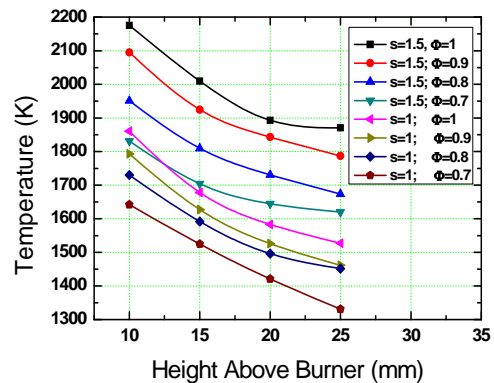


Figure 6. The height above burner dependence of the temperature measured in different flames.

The HAB dependence of the temperature measured in different flames is plotted in Fig. 6. It can be seen that the temperature in the burned gas drops quickly with the increasing HAB. This is mainly owing to the small size of the quartz burner. So when using this burner as a calibration source, one has to pay attention to the HAB, since the temperature is sensitive to that.

The standard deviation of 3 sets of experiments was summarized in Tab. 2. And it can be seen that the maximum error is $\sim 50 \text{ K}$ in this paper.

Table 2. Standard deviation of 3 sets of experiments for different equivalence ratio and air flow rate.

Equivalence Ratio	Standard Deviation (K)	
	Speed= 1 m/s	Speed= 1.5 m/s
0.7	32.9	45.8
0.8	5.5	29.4
0.9	16.1	55.3
1.0	57.7	31.5

5. Summary

A handy multi-jet quartz burner has been demonstrated, as well as the laminar premixed methane/air flames on it. Rayleigh scattering thermometry technique has been adopted to measure the temperature. The flames are found to be close to adiabatic flame. The burned gas regions of these flames provide handy calibration flames in reasonably small scale to be available to laser labs for not only the calibration before practical measurements and also testing for new laser techniques in the developing stage.

Acknowledgements

This work has been financed by SSF (Swedish Foundation for Strategic Research) and the Swedish Energy Agency through CECOST (Centre for Combustion Science and Technology) and VR (Swedish Research Council).

References

- [1] K. Kohse-höinghaus and J. B. Jeffries, eds., applied combustion diagnostics, Combustion: An international series, Taylor & Francis, New York, 2002.
- [2] J. Nygren, J. Engstrom, J. Walewski, C. F. Kaminski, and M. Alden, Measurement Science & Technology 12 (2001) 1294.
- [3] S. Prucker, W. Meier, and W. Stricker, Review of Scientific Instruments 65 (1994) 2908.
- [4] W. D. Kulatilaka, R. P. Lucht, S. F. Hanna, and V. R. Katta, Combustion and Flame 137 (2004) 523.
- [5] G. Hartung, J. Hult, and C. F. Kaminski, Measurement Science & Technology 17 (2006) 2485.
- [6] A. D. P. Shardanand; Rao, NASA Tech. Rep. TN D-8442 (National Aeronautics and Space Administration, Washington, D.C. (1977)
- [7] I. Namer and R. W. Schefer, Experiments in Fluids 3 (1985) 1.
- [8] J. A. Sutton and J. F. Driscoll, Experiments in Fluids 41 (2006) 603.